Thermal Effects During Plastic Flow in Nickel-Base Superalloys

BRUNO LISIECKI*, LADISLAS KUBIN*, YURI ESTRIN - *CNRS-ONERA (OM), Laboratoire d'Etude des Microstructures, Chatillon, France - **Technishe Universität Hamburg-Harburg, Werkstoffphysik und -technologie, Hamburg, Germany.**

Abstract

Two cases of significant adiabatic heating during plastic flow are examined. Both concern nickel base superalloys. In a single crystal of AM3 superalloy deformed with a moderate strain rate at room temperature, a high rate of energy dissipation stems from strain localization. A local temperature increment of about 120 K was measured by infra-red thermography. In a MA 6000 superalloy deformed at 1123 K, a significant homogeneous temperature increase (70 K) stems from a high rate of uniform deformation. In both cases, the adiabatic approximation allows an estimate of the temperature increments with good accuracy.

Riassunto

Vengono esaminati due casi di riscaldamento adiabatico significativo che si è verificato durante il flusso plastico. Si trattava in ciascun caso di una superlega a base di nichel. In un unico cristallo di superlega AM3 deformata a T.A. e ad una velocità moderata di tensione, la localizzazione della tensione genera un'alta velocità di dissipazione d'energia. La termografia a I.R. ha rivelato un incremento locale di circa 120 K. In una superlega MA 6000 deformata a 1123 K, l'alta velocità di deformazione uniforme genera un aumento significativo ed omogeneo di 70 K. In entrambi i casi, una stima sufficientemente precisa degli incrementi di temperatura può essere ricavata dall'approssimazione adiabatica.

Introduction

The process of plastic deformation of metallic materials is highly dissipative, most of the mechanical work being transformed into heat. The resulting increase in temperature is, however, negligible, except when the rate of energy dissipation is very large. In the present communication, two such situations are investigated, both with nickel-base superalloys. AM3 is a new γ/γ' superalloy elaborated by ONERA. In that case, a high rate of energy dissipation resulted from *strain localization* due to the shearing of particles of the ordered γ' phase [1]. In the case of the superalloy MA 6000 deformed at 1123 K, a significant *homogeneous heating* of the specimen was obtained due to a high imposed strain rate ($0.3\ s^{-1}$). Since the mechanical properties of MA 6000 are temperature dependent (in contrast to the AM3 superalloy around room temperature), the heat release brings about a substantial softening [2,3].

For both cases, the temperature increment will be estimated assuming that heating is adiabatic. This assumption will be justified by comparison with experiment, in particular with the results obtained by infra-red thermography on the AM3 superalloy. In the case of MA 6000, the validity of this assumption will also be substantiated theoretically.

Thermal Effects in AM3 Superalloy

Single crystals of AM3 oriented along the [011] axis were deformed in tension at room temperature with the strain rate of $1.3 \cdot 10^{-4}\ s^{-1}$. The deformation curves were shown to be serrated. Each serration was accompanied by an audible click and was associated with the formation of a glide band shearing the whole crystal along a {111} slip plane (Fig. 1). The infra-red emission of the specimen was measured with the help of a commercial infra-red camera, AGEMA 880. Simultaneously, the stress-strain curve was recorded and the specimen surface was imaged by a video camera. This allowed the identification of stress serrations and the associated shear bands as well as the infra-red bursts. As the stress drops occurred within a very short time (presumably of the order of $10^{-5}\ s^{-1}$), the infra-red camera was operated in the line scanning mode. In this mode, a line perpendicular to the specimen axis is scanned with a frequency of $2500\ s^{-1}$. An infra-red record of a stress drop event performed in such conditions is shown in Fig. 2.

Fig. 3 is the corresponding thermogram in which the digitized infra-red signal N, which is proportional to temperature, is plotted as a function of time. From the surface video recording, the shear band was determined to lie about 1 mm above the line observed. This explains the time dependence of

the temperature recorded on Fig. 2. It took 0.32 s for the temperature peak to reach the location of the line. The maximum temperature increment there was $\Delta T_{max} = 0.92$ K. It was followed by a slow decrease as heat propagated by conduction along the specimen axis.

To analyze this result, we assume that a temperature burst ΔT_o is instantaneously generated inside a band of width 2a, the specimen temperature outside the band being $T_o = 300$ K. The solution of the heat conduction equation with such initial conditions and for uniaxial geometry [4] yields for the coordinate and time dependent temperature increment.

$$\Delta T = (\Delta T_o/2)\left[\mathrm{Erf}\left((a-x)/(4\varkappa t)^{1/2}\right) + \mathrm{Erf}\left((a+x)/(4\varkappa t)^{1/2}\right)\right] \tag{1}$$

where $\varkappa$ is the thermal diffusivity, x is the distance from the center of the band measured along the specimen axis, and $\mathrm{Erf}(u) = \int_o^u \exp(-v^2)\,dv$ is the error function. To estimate ΔT_o, we make use of the fact that the value of time at which the maximum temperature increment is reached on the line surveyed is measured with good precision (Fig. 3). By setting $d\Delta T/dt = 0$ one obtains with eq. (1)

$$t(\Delta T_{max}) = (ax/\varkappa)/\ln[(x+a)/(x-a)] \tag{2}$$

The band width was measured in a scanning electron microscope after the deformation test to yield $2a = 40$ μm. From Fig. 3, we have $0.309\ \mathrm{s} < t(\Delta t_{max}) < 0.336$ s. With the help of the same infra-red device, the thermal diffusivity of AM3, $\varkappa$, was measured at room temperature to be $2.4 \cdot 10^{-6}\ \mathrm{m^2 s^{-1}}$. This value is pretty low, about two orders of magnitude smaller than for a good thermal conductor. From eq. (2), we obtain $1.216\ \mathrm{mm} < x < 1.267$ mm. Substituting into eq. (1) the two values delimitating the interval in which x must lie yields two time dependences of ΔT shown in Fig. 4. Both curves pass through the point $\Delta T = \Delta T_{max} = 0.92$ K, $t = t(\Delta T_{max})$. The corresponding initial temperature increment ΔT_o in the glide plane has the values 116 K and 121 K, respectively. Accordingly, the initial temperature rise in the glide band is evaluated to lie in the interval $116\ \mathrm{K} < \Delta T_o < 121$ K.

The above estimate is to be compared with that obtained in the adiabatic approximation. Assuming that a fraction α of the mechanical work per unit volume of the glide band, $\sigma_o \Delta\varepsilon_p$, associated with a plastic strain burst $\Delta\varepsilon_p$, is released as heat, the adiabatic temperature increment is evaluated as

$$\Delta T_{ad} = \alpha \sigma_o \Delta\varepsilon_p / \varrho c_p \tag{3}$$

Here σ_p is the stress at which a stress drop and the associated plastic strain burst occur ($\sigma_o = 925$ MPa in the case under consideration); $\varrho = 8.25 \cdot 10^3\ \mathrm{kg/m^3}$ is the density of AM3 and c_p is its heat capacity at constant pressure. For the present evaluation the value of $c_p = 410\ \mathrm{Jkg^{-1}deg^{-1}}$ for a related superalloy, AM1, is utilized. The plastic strain burst $\Delta\varepsilon_p$ is obtained from the "machine equation" relating the decrement of the elastic strain, $\Delta\sigma/M$, to the increment of the plastic one:

$$\Delta\sigma/M = (2a/L)\,\Delta\varepsilon_p \tag{4}$$

Here M denotes the combined elastic modulus of the specimen and the testing machine ($M = 30$ GPa) and L is the specimen gauge length. The factor 2a/L on the right-hand side of the equation accounts for the fact that plastic strain burst is localized within a band of width 2a. As already mentioned, the stress drop duration is so short that the specimen elongation due to applied strain rate could be disregarded in the machine equation. Estimation of ΔT_{ad} with the aid of eqs. (3) and (4) for the measured stress decrement $\Delta\sigma = 40$ MPa and $2a/L = 1.83 \cdot 10^{-3}$ (meaning a very strong localization) yields, with $0.85 < \alpha < 0.9$,

$$142\ \mathrm{K} < \Delta T_{ad} < 150\ \mathrm{K} \tag{5}$$

These values are slightly in excess of those estimated above from the infra-red thermography experiment, but the agreement is satisfactory.

The above example confirms reasonable applicability of the adiabatic approximation. The adiabaticity of heating in this case owes to strong localization of the plastic event, to a high stress level in AM3 as well as to its poor thermal diffusivity. It should be noted that the plastic flow properties of this alloy are almost temperature independent in the room temperature range, so that the thermal effects are decoupled from the mechanical effects. This is no longer the case with the next alloy considered.

Thermomechanical Effects in Inconel MA 6000

The effect of homogeneous heating and associated strain softening is illustrated by the experimental results obtained by Singer and Gessinger [2] on the superalloy Inconel MA 6000 deformed in compression with high nominal strain rate $\dot{\varepsilon}_a = 0.3\ s^{-1}$. The experimental stress vs. strain curve obtained at 1123 K (850°C) is shown on Fig. 5. The observed decrease in stress was attributed by the authors to thermal softening due to adiabatic heating, as a sample temperature of 1193 K (920°C) was measured at the end of the test. (cf. Fig. 5).

To check the accuracy of the adiabaticity hypothesis, we first consider the pertinent time scales involved [3]. The duration of deformation experiment, $t_e = 2.04$ s, is to be compared with two characteristic times which determine the rate of heat removal. One is the time needed for temperature equalization within the specimen by heat diffusion in the bulk: $t_{bulk} = d^2/4\varkappa$. Here d is the larger of the two quantities: the active glide band spacing or the specimen radius R. The other time scale is given by the rate of heat transfer to the thermal bath through the specimen surface: $t_{surface} = (\varrho c_p/h)(A/P)$. Here h is the coefficient of surface heat transfer; A and P denote the cross-sectional area and circumference, respectively. For the cylindrical specimen geometry used, A/P = R/2. Numerical values of the parameters entering the two heat removal times are summarized in Table 1, the value of h being an order-of-magnitude estimate obtained from Refs. 4 and 5. Then, with $d \leq R$, the following inequalities follow:

$$t_{bulk} \leq 0.7\ s < t_e \leq t_{surface} \approx 90\ s. \tag{6}$$

TABLE 1 - Numerical values for the thermal, geometrical and mechanical parameters of MA 6000.

R, m	ϱc_p, $Jm^{-3}K^{-1}$	$\varkappa$, m^2s^{-1}	h, $Wm^{-2}K^{-1}$	T_o, K	m	β
$4\ 10^{-3}$	$4.6 \cdot 10^6$	$5.76 \cdot 10^{-6}$	10^2	1123	0.4	30

These inequalities signify two important properties:

(i) As the time of equalization of temperature within the specimen is small as compared with the time of surface heat transfer, the temperature can be considered uniform throughout the specimen.

(ii) Since the heat transfer time is larte as compared to the test duration, the heat generated is stored within the specimen throughout the test duration so that heating can be considered to be adiabatic.

Within the adiabatic approximation, the interplay between thermal and mechanical effects can be expressed through a set of two coupled equations:

$$c_p \varrho \dot{T} = \alpha \sigma \dot{\varepsilon}_a,\ \dot{\varepsilon}_a = A\sigma^{1/m} \exp(-\beta T_o/T) \tag{7}$$

The first of the two equations expresses the energy balance under adiabaticity conditions. Here σ is the flow stress and the applied strain rate, $\dot{\varepsilon}_a$, is nearly equal to the plastic strain rate beyond the yield point. The second equation expresses the thermally activated nature of plastic flow. Its form was empirically determined by Singer and Gessinger [2]. In this equation m is nondimensional strain rate sensitivity of the flow stress, A is a constant which is eliminated by setting $T = T_o$ at the yield stress $\sigma = \sigma_y$. The exponential factor incorporates the influence of temperature on nickel self-diffusion in Ni-Cr alloys. The values of m and β are contained in Table 1.

The set of eqs. (7) is readily solved yielding

$$\sigma = \sigma_y[1 + (\alpha m \beta \sigma_y \dot{\varepsilon}_a t / c_p \varrho T_o)]^{-1}, \quad T - T_o = (T_o/m\beta)\ln(\sigma_y/\sigma) \tag{8}$$

After transforming the engineering strain $\dot{\varepsilon}_a t$ into the true strain rate, the stress vs. true strain curve is readily calculated with the help of the first of eqs. (8), using the parameter values from Table 1. The resulting curve matches the experimental one almost perfectly (Fig. 5), without the use of any adjustable parameter. At the end of the test, the calculation yield the values of 371 MPa for stress and 1192 K for specimen temperature (i.e., a temperature increase of 69 K), to be compared with the measured values of 387 MPa and 1193 K, respectively. A more detailed examination of this problem shows [3] that the observed behaviour is actually a transient. The system tends towards a stable steady state, but with a transient time larger than the duration of the deformation test.

Conclusions

The two experimental examples considered illustrate the usefulness of the adiabatic approximation in evaluating the heating the heating effects during plastic flow. The adiabaticity stems from high degree of strain localization in one case and from high speed of uniform deformation in the other one. The model of adiabatic heating is, however, not of general applicability. A full analysis of thermomechanical coupling yielding the steady state temperature increments for both homogeneous and strongly localized heat generation was given in Refs. 6 and 7. In addition, the conditions for the onset of thermomechanical instability of plastic flow at very low temperatures were suggested.

The experimental manifestations of the heat generation effect considered in the present paper demonstrate that the adiabatic approximation is fully justified in both cases examined. A consequence is that the quantities favouring strain softening in the MA 6000 superalloy can be identified using a simple analytical expression. In the case of the AM3 superalloy, it was demonstrated that infra-red thermography is a powerful technique for investigating temperature transients during plastic flow.

Acknowledgements

The authors are wish to thank to P. Caron (ONERA-OM) and P. Levesque (ONERA-DES) for their contribution to the experiments on the AM3 superalloys. Financial support from DAAD (Germany) and ANRT (France) through the PROCOPE program is gratefully acknowledged.

References

[1] Lisiecki, B., P. Caron and L.P. Kubin. In Rosen (Ed.), *Strength of Metals and Alloys*, (Proc. ICSMA 9, Haifa, Aug. 1991), Pergamon Press, Oxford, 1991, to be published.

[2] Singer, R.F., and G.H. Gessinger. *Met. Trans., 13A* (1982), 146.
[3] Estrin, Y., and L.P. Kubin. Thermal softening of Inconel MA 6000 alloy. *Mat. Sci. Eng., 57* (1983), 137-142.
[4] Carslaw, H.S., and J.C. Jaeger. *Conduction of Heat in Solids*, Clarendon Press, Oxford, pp. 54 and 366.
[5] Rosenqvist, T., *Principles of Extractive Metallurgy*, Mc Graw-Hill, New-York, Sections 6.5 and 6.8.
[6] Estrin Y., and L.P. Kubin. Thermomechanical instabilities of low temperature plastic flow. In O. Brulin and R.K.T. Hsieh (Eds.), *Continuum Models of Discrete Systems 4*, North-Holland Publ. Co., Amsterdam, pp. 13-20.
[7] Molinari, A., Y. Estrin, and D. Dudzinski, Thermomechanical instability associated with heat release during plastic flow. *Int. J. Plasticity*, to be published.

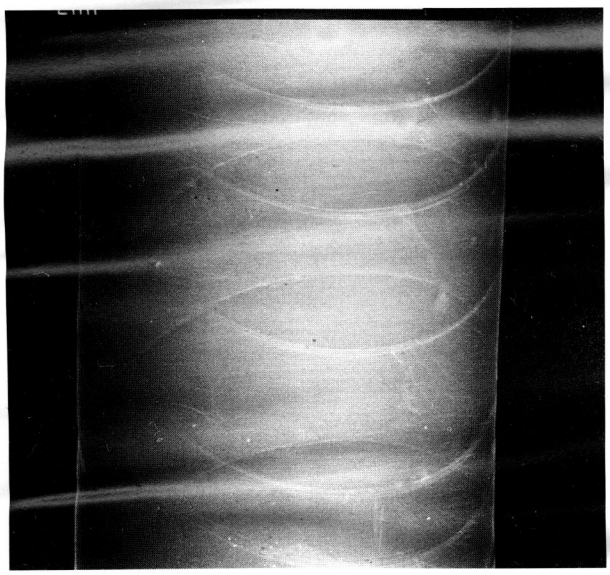

Fig. 1:
Scanning electron microscopy observation of a single crystal of AM3 after deformation at room temperature. The specimen axis is parallel to [011] and the glide bands are along one of the two potentially active {111} slip planes, x22.6.

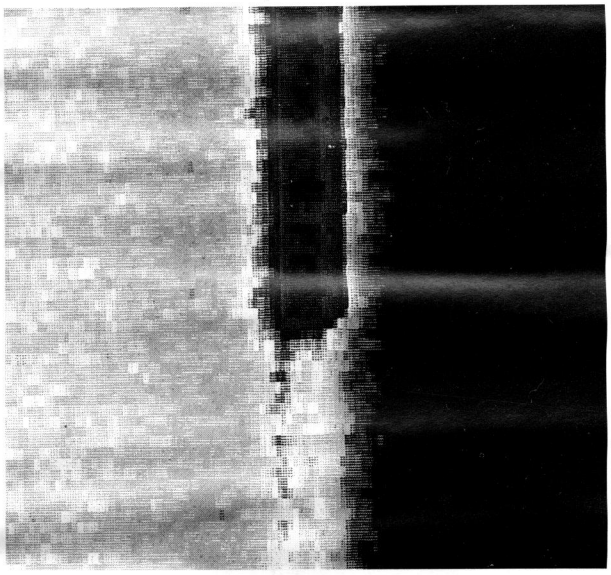

Fig. 2:
A thermal image in the line scanning mode. The specimen is visualized by two vertical bars; time increases from bottom to top, with an interval of 400 μs between lines. Near the middle of the image the colour of the specimen changes (from yellow to blue in the original picture), which indicates an increase of temperature.

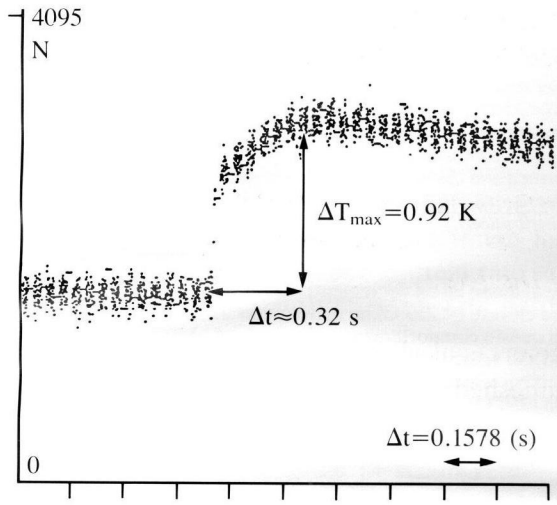

Fig. 3:
A thermogram N vs. time obtained from the thermal image of Fig. 2. N is the digitized infrared signal, which is proportional to temperature.

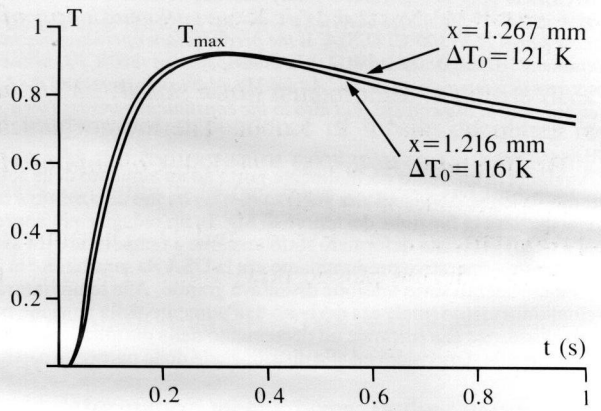

Fig. 4:
Temperature vs. time diagram for two possible locations of the monitored line with respect to the glide band. ΔT_o is the corresponding initial temperature increment.

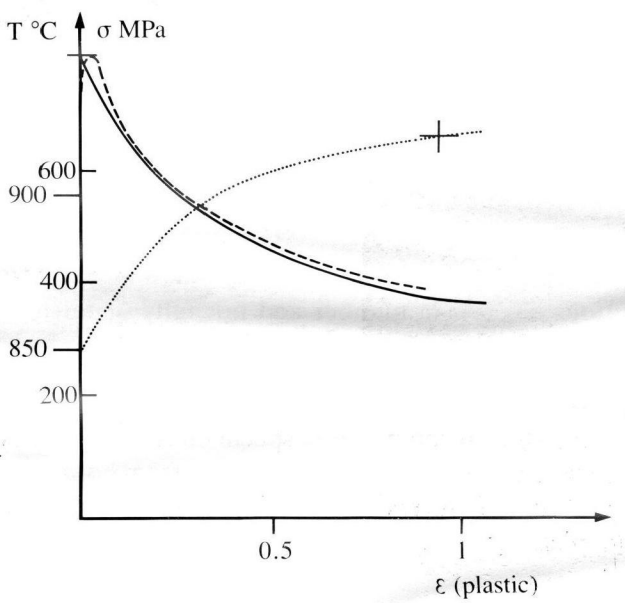

Fig. 5:
..... Experimental stress-strain curve for Inconel MA 6000 superalloy, after Singer and Gessinger [3].
_____ Present calculation of the stress-strain curve.
_ _ _ _ Present calculation of the temperature T within the specimen.
\+ Experimental value of temperature at the end of the test [3].